https://doi.org/10.5194/esurf-2020-37
Preprint. Discussion started: 18 June 2020

Structural variations in basal decollement and internal deformation of the Lesser Himalayan Duplex trigger landscape morphology in NW Himalayan interiors

Saptarshi Dey[1], Rasmus Thiede[2], Arindam Biswas[3], Pritha Chakravarti[1], and Vikrant Jain[1]

[1]*Earth Science Discipline, IIT Gandhinagar, Gandhinagar-382355, India.*

[2]*Institute of Geosciences, Christian Albrechts University of Kiel, Kiel-24118, Germany.*

[3] *Department of Applied Geology, IIT-ISM Dhanbad, Jharkhand-826004, India.*

Corresponding author

Saptarshi Dey

saptarshi.dey@iitgn.ac.in

Abstract

The Kishtwar Window (KW) of the NW Himalaya exposes the northwestern termination of the orogen-parallel anticlinal stack of thrust nappes, termed as the Lesser Himalayan Duplex and its evolution portrays rapid exhumation at least over the last 2-3 Myr. However, speculations remain if it still actively deforming. Here we combine morphometric analyses with structural and field evidences to describe the spatial pattern of internal deformation of the duplex. We suggest that the variations in the geometry of the basal décollement, the Main Himalayan Thrust (MHT) and internal faulting within the duplex define the observed neotectonic deformation. We recognize two significant steep stream segments/ knickzones, one in center of the window, and a second one along its western margin, which we relate to fault-ramps emerging from the MHT. The larger of the knickzones, in the core of the window, show an increase in the angle of

foliations towards downstream. Highly-fractured and folded rocks at the base of the steep stream segment, suggest internal deformation of the duplex, possibly linked to surface-breaking thrust fault-ramp at the core of the duplex. The second steepened knickzone coincides with the western margin of the window and is identified by a narrow channel through a comparatively weaker bedrock gorge. Summarizing our findings, we favor a structural and active tectonic control on the growth of the duplex even over geomorphic timescales. Corroborating with previous studies, we suggest that the differential uplift and growth of the duplex is linked to several flat-ramp structures along the MHT.

Keywords

Steepness index, knickzone, rock strength, Lesser Himalayan Duplex, Main Himalayan Thrust.

1. Introduction

Protracted convergence between the Indian and the Eurasian plate resulted into the growth and evolution of the Himalayan orogen and temporal in-sequence formation of the Southern Tibetan Detachment System (STDS), the Main Central Thrust (MCT), the Main Boundary Thrust (MBT) and the Main Frontal Thrust (MFT) towards the south (Yin and Harrison, 2000; Yin, 2006; Mukherjee, 2013). All these fault-zones emerge from a low-angle basal decollement, the Main Himalayan Thrust (MHT), established in the late Miocene (Vannay et al., 2004) and forming the base of the Himalayan orogenic wedge (Ni and Barazangi, 1984; Nabelek et al., 2009; Avouac et al., 2016).

https://doi.org/10.5194/esurf-2020-37
Preprint. Discussion started: 18 June 2020

Majority of scientists have favored that the late Pleistocene-Holocene shortening of the Himalaya is mostly accommodated within the southern margin of the wedge, i.e., the Sub-Himalaya (morphotectonic segment in between the MBT and the MFT) (Wesnousky et al., 1999; Lave and Avouac, 2000; Burgess et al., 2012; Thakur et al., 2014; Mukherjee, 2015; Vassalo et al., 2015; Dey et al., 2016; Dey et al., 2018). The statement above implies that the northerly thrusts, i.e., the MBT and the brittle faults exposed in the vicinity of the southern margin of the Higher Himalaya, are considered inactive and not contributing to the growth and total shortening of the Himalaya since at least late Pleistocene. However, in recent years, several studies focused on the low-Temperature thermochronological data and thermal modeling of the interiors of the NW Himalaya have raised questions on the statement above. The recent studies suggested that 10-15% of the total Quaternary shortening has been accommodated within the interiors of the Himalaya as out-of-sequence deformation, i.e., in hanging wall of the MBT or other structures (Thiede et al., 2004; Deeken et al., 2011; Thiede et al., 2017; Gavillot et al., 2018) (*Fig. S1*). Overall, the out-of-sequence deformation of the Himalayan wedge has been explained by two end-member models. One of them favored reactivation of the MCT (Wobus et al., 2003), while the other tried to explain all changes along the southern margin of the Higher Himalaya with a major ramp triggering deformation along the MHT (Bollinger et al., 2006; Herman et al., 2010; Robert et al., 2009). Landscape evolution models, structural analysis and thermochronological data from the interior of the Himalaya favor that the Lesser Himalaya has formed a duplex at the base of the southern Himalayan front by sustained internal deformation since late Miocene (Decelles et al., 2001; Mitra et al., 2010; Robinson and Martin, 2014). Growth of the duplex resulted into the uplift of the Higher Himalaya forming the major orographic barrier of the orogen. The Kishtwar Window (KW) in the NW Himalaya represents the northwestern

https://doi.org/10.5194/esurf-2020-37
Preprint. Discussion started: 18 June 2020

termination of the Lesser Himalayan Duplex (LHD). While most of the published cross-sections of the Himalayan orogen today recognize the duplex (Webb et al., 2011; Mitra et al., 2010; DeCelles et al., 2001), usually very little or no data are available on how the deformation is spatially as well as temporally distributed and most importantly, whether the duplex is active over timescales shorter than a million year.

The pioneering low-temperature thermochron study by Kumar et al., (1995) portrayed the first orogen-perpendicular sampling traverse extending from the Kishtwar tectonic Window over the Zanskar Range. More recent studies link the evolution of the KW to the growth of a Lesser Himalayan Duplex structure (Gavillot et al., 2018), surrounded by the Miocene MCT shear zone along the base of the High Himalayan Crystalline, locally named as the Kishtwar Thrust (KT). Thermochronological constraints suggest higher rates of exhumation within the window (3.2-3.6 $mm.a^{-1}$) (Gavillot et al., 2018), corroborating well with similar thermochron-based findings from the of the Kullu-Rampur window along the Beas Stübner et al., (2018) and Sutlej valley (Jain et al., 2000; Vannay et al., 2004; Thiede et al., 2004) over the Quaternary timescale. In contrast, geodetic shortening rates, lack spatial resolution and only capture inter-seismic deformation (Banerjee and Burgmann, 2002; Kundu et al., 2014), and there exists no chronological data to provide information on ongoing tectonic activity in the interiors of the Himalaya over intermediate timescales. Therefore, to understand the 10^3-10^4-year timescale neotectonic evolution, either we have to have geological field evidence, chronologically-constrained geomorphic markers or at least have a rigorous morphometric analysis of potential study areas, such as the KW.

Documenting over-steepened longitudinal river profiles along the southern margin of the Higher Himalaya was pioneered by Seeber and Gornitz (1983), who related that to Quaternary

https://doi.org/10.5194/esurf-2020-37
Preprint. Discussion started: 18 June 2020

internal deformation and recent uplift. They used longitudinal stream profiles and stream-length index and identified unadjusted and steep stream segments at the transition from the Lesser to the Higher Himalaya along sixteen major Himalayan rivers, including the Chenab river passing through the Kishtwar-Jammu region. Similarly, a study by Nennewitz et al., (2018) also portrayed morphometric indices (basinwide steepness indices and topographic relief) across a large part of the NW Himalaya. Though the resolution of the analyses was coarse, the first-order results encourage us to explore the large drainage networks over the prospect study areas in much more detail and with a terrain data having finer resolution than 30m SRTM DEM used before.

Another pivotal question on the Himalayan wedge kinematics is about the structural pattern of the basal decollement. Based on the large-scale basinwide morphometric analysis, Nennewitz et al., (2018) have proposed that the million-year-timescale shortening achieved in the interior of the Himalaya near the Sutlej-Beas area in the eastern Himachal Pradesh is caused by accentuated rock uplift over a ramp at a mid-crustal depth of ~ 8-25 km on the MHT. In contrast, studies from the Dhauladhar Range in the northwestern Himalaya hints the presence of deep-seated crustal ramp on the MBT and yielded a shortening rate of 1.5-3 mm a^{-1} across the MBT over the last 8 Ma and absence of mid-crustal ramp (Thiede et al., 2017). However, it is still unclear whether this proposed ramp on the MHT is laterally continuous or is interrupted in the far western sectors of the Ravi-Chamba region in the western Himachal Pradesh and Jammu region. Gavillot et al. (2018) recently presented an orogen-perpendicular balanced cross-section of the Chenab region extending ~160 km inside the MFT, which favors the existence of a mid-crustal ramp beneath the KW. Their suggestion is in agreement with very young AFT cooling ages (1-3 Ma) (Kumar et al., 1995) in the window and previous documentation of structural deformation styles described in DiPietro and Pogue (2004), Yin (2006) and Searle et al., (2007). Previous work, however, lacks field evidence, as well as details about of active deformation. The thermochronological control is also restricted to very limited stretches along the Chenab River and hardly covers the entire KW. Therefore, the interpretation of deformation pattern based on exhumation rates is not very well constrained. However, the high Quaternary exhumation rates from the KW motivated us to study the KW and the surroundings in detail.

In this study, we will focus on few long-standing questions on Himalayan neotectonic evolution, which are-

1. What is the spatial extent of neotectonic deformation, if any, in the interiors of the Himalaya?

2. What is the role of the Lesser Himalayan duplex in defining the morphology of the Himalayan interiors?

3. How reliably we can infer about sub-surface structural variations of the orogenic wedge by analyzing the terrain morphology?

To address these questions, we adopted a combination of methods such as morphometric analysis using high-resolution digital elevation models, field observation on rock type, structural variations as well as rock strength data collection and, analysis of satellite images to assess the spatial distribution of the late Quaternary deformation of the KW and surroundings (Fig.1). Our aim was to test if the landscape morphology can be explained by changes in the basal decollement and associated active structures, likewise it has been done in the neighboring sectors of the Himalaya (Fig.1). We have used 12.5m ALOS PALSAR DEM and LANDSAT satellite imagery for various morphometric analyses such as longitudinal stream profiles, basinwide

https://doi.org/10.5194/esurf-2020-37
Preprint. Discussion started: 18 June 2020

normalized steepness indices and channel width measurement. We calculated specific stream power of selected stretches within the study area and used it as a proxy of fluvial incision. We combined the results with field observation, field-collected data on bedrock structural styles and rock strength data by using hand-held rebound hammer to investigate the spatial distribution of neotectonic deformation in the vicinity of the KW. Our morphometric results document that the regional distribution of faulting is concentrated in the core of the window and along the western margin of the window, and indicated that faulting within and growth of the Lesser Himalayan Duplex are controlling deformation of the Himalayan interior and uplift of High Himalaya in its hanging wall. With this study, we put new insights on the structural variations within the NW Himalayan interiors and spatial distribution of neotectonic evolution of the Himalayan orogen over the geomorphic timescale of 10^4-10^5 years.

2. Geological background

The orogenic growth of the Himalaya, resulted an overall in-sequence development of the orogen-scale fault systems which broadly define the morphotectonic sectors of the orogen (*fig. S1*). Notable among those sectors, the Higher Himalaya is bordered by the MCT in the south and is comprised of high-grade metasediments, Higher Himalayan Crystalline Sequence (HHCS) and Ordovician granite intrusives (Yin and Harrison, 2000). The Low-grade metasediments (quartzites, phyllites, schists, slates) of the Proterozoic Lesser Himalayan sequence are exposed between the MCT in the north and MBT in the south. The Lesser Himalayan domain is narrow (4-15 km) in the NW Himalaya except where it is exposed in the form of tectonic windows (Kishtwar window, Kullu-Rampur window etc.) in the western Himalaya (Steck, 2003). The

https://doi.org/10.5194/esurf-2020-37
Preprint. Discussion started: 18 June 2020

Sub-Himalayan fold-and-thrust belt lying to the south of the MBT is tectonically the most active sector since the late Quaternary (Thakur et al., 2014; Vignon et al., 2016).

Near the southwest corner of our study area, Proterozoic low-grade Lesser Himalayan metasediments are thrust over the Tertiary Sub-Himalayan sediments along the MBT (Wadia, 1934; Thakur, 1992). Near the Chenab region, Apatite U-Th/He ages suggest that cooling and exhumation related to faulting along the MBT thrust sheet initiated before ~5 ± 3 Ma (Kumar et al., 1995). Geomorphic data obtained across the MBT in Kashmir Himalaya suggest that MBT has not been reactivated for the last 14-17 ka (Vassallo et al., 2015). In the NW Himalaya, the Lesser Himalayan sequence (LHS) exposed between the MBT and the MCT is characterized by a < 10 km-wide zone of sheared schists, slates, quartzites, phyllites and Proterozoic intrusive granite bodies (Bhatia and Bhatia, 1973; Thakur, 1992; Steck, 2003). The LHS is bounded by the MCT shear zone in the hanging wall. The MCT hanging wall forms highly deformed nappe exposing lower and higher Haimantas, which are related to the Higher Himalayan Crystalline Sequence (HHCS) (Bhatia and Bhatia, 1973; Thakur, 1992; Yin and Harrison, 2000; Searle et al., 2007). Nearly 40 km NE of the frontal MCT shear zone, MCT fault zone is re-exposed in the vicinity of KW is called the Kishtwar Thrust (KT) (Ul Haq et al., 2019) (*fig. 1*). Within the KW, Lesser Himalayan Rampur quartzites, low-grade mica schists and phyllites along with the granite intrusives are exposed (Steck, 2003; DiPietro and Pogue, 2004; Yin, 2006; Gavillot et al., 2018). (*Fig. 2a*). KW exposes a stack of LHS nappes in the footwall of the MCT (in this case, KT) which is related to the Lesser Himalayan Duplex (LHD), characteristic of the central Himalaya (Decelles et al., 2001). Regionally balanced cross-sections (DiPietro and Pogue, 2004; Searle et al., 2007; Gavillot et al., 2018) suggest that the Himalayan wedge is bounded at the base by décollement, named the MHT. Sub-surface structural formations beneath the KW is not well-

https://doi.org/10.5194/esurf-2020-37
Preprint. Discussion started: 18 June 2020

constrained. A recent study by Gavillot et al., (2018) propose the existence of two mid-crustal ramp segments beneath the KW, viz., MCR-1 and MCR-2 (*fig. S2*). Based on thermochronological constraints, Gavillot et al. (2018) and Kumar et al., (1995), proposed that the core of the window is exhumed with rates > 1 $mm.a^{-1}$ during the Quaternary, at a higher rate when compared to the surroundings.

3. Methods of morphometric analysis and field data collection

3.1. Morphometry

For conducting the morphometric analysis, we have used 12.5m ALOS-PALSAR DEM data (high resolution terrain-corrected). This DEM data has lesser issues with artifacts and noises than 30m SRTM data, which fails to capture the drainage network properly in areas populated by narrow channel gorges.

3.1.1. Drainage network extraction

The drainage network and the longitudinal stream profiles were extracted using the Topographic Analysis Kit toolbox (Forte and Whipple, 2019). An equivalent of 10-pixel smoothing of the raw DEM data has been applied to remove noises from the DEM. The longitudinal stream profile of the Chenab trunk stream was processed with the Topotoolbox 'Knickpointfinder' tool (Schwanghart and Scherler, 2014). Several jumps/ kinks in the longitudinal profile are seen and those are marked as knickpoints (Fig.2a). A 30m tolerance threshold was applied to extract only the major knickpoints.

3.1.2. Basinwide normalized steepness indices

https://doi.org/10.5194/esurf-2020-37
Preprint. Discussion started: 18 June 2020

Global observations across a broad spectrum of tectonic and climatic regimes have revealed a power-law scaling between the local river gradient and upstream contributing area:

$$S = ks.\ A^{-\theta} \qquad (1)$$

where S is the stream gradient (m/m), ks is the steepness index ($m^{2\theta}$), A is the upstream drainage area (m^2), and θ is the concavity index (Flint, 1974; Whipple and Tucker, 1999). Normalized steepness-index values (k_{sn}) are steepness indices calculated using a reference concavity value (θ_{ref}), which is useful to compare steepness-indices of different river systems (Wobus et al., 2006). We extracted the k_{sn} values in the study area using the ArcGIS and MATLAB-supported Topographic Analysis Toolkit (Forte and Whipple, 2019) following the procedure of Wobus et al. (2006). We performed an automated k_{sn} extraction using a critical area of 10^6 m^2 for assigning the channel head, a smoothing window of 500 m, a θ_{ref} of 0.45, and an auto-k_{sn} window of 250 m for calculating k_{sn} values. The slope-breaks, known as the knickpoints (sometimes referred to as knickzones if it is manifested by a series of rapids instead of a single sharp break in profile), were allocated by comparing the change of slope along the distance-elevation plot (Fig.2a). The threshold 'dz' value (projected stream offset across a knickpoint) for this study is 30m. Basinwide mean k_{sn} values are plotted using a 1000 km^2 threshold catchment area (Fig. 3a).

Identification of the knickpoints/ knickzones and their relationship with the rock-types as well as with existing structures are necessary to understand the causal mechanism of the respective knickpoints/ knickzones. Knickpoints/(zones) can be generated by lithological, tectonic and structural control. Lithological knickpoints are stationary and anchored at the transition from the soft-to-hard substrate. The tectonic knickpoints originate at the active tectonic boundary and migrate upstream with time. Structural variations, such as ramp-flat geometry of any emerging thrust may cause a quasistatic knickpoint at the transition of the flat-to-ramp of the fault. In such cases, the ramp segment is characterized by higher steepness than the flat segment and often the ramp is characterized by a sequence of rapids, forming a wide knickzone, instead of a single knickpoint.

3.1.3. Channel Width

Channel width is a parameter of assessment of lateral erosion/incision through bedrocks of equivalent strength (Turowski, 2009). The channel width of the Chenab trunk stream within the elevation range of 600 to 2200 m above the MSL was derived by manual selection and digitization of the channel banks using the Google Earth Digital Globe imagery (http://www.digitalglobe.com/) of minimum 3.2 m spatial resolution. We used the shortest distance between the two banks as the channel width. We rejected areas having largely unparallel channel-banks as that would bias the result. We used a 50 m step between two consecutive points for channel width determination. Twenty point-averaged channel width data along with elevation of the riverbed, is shown in *Fig.3b*.

3.1.4. Specific stream power (SSP) calculation

Specific stream power has often been used as a proxy of fluvial incision or differential uplift along the channel (Royden and Perron, 2013; Whipple and Tucker, 1999). Areas of higher uplift/incision are characterized by transient increase in the specific stream power. Channel slope and channel width data were used to analyse the corresponding changes in the specific stream power (SSP) from upstream of the gorge area to the gorge reaches (Bagnold, 1966). The SSP (ω) was estimated using the following equation –

$$\omega = \gamma . Q . s / w \qquad \text{(Eq. 1)}$$

https://doi.org/10.5194/esurf-2020-37
Preprint. Discussion started: 18 June 2020

Where, γ - unit weight of water, Q – water discharge, s – energy slope considered equivalent to the channel slope; w – channel width. SSP data from selected stretches are shown in Table 1.

3.2. Field data collection

3.2.1. Structural data

We measured the strike and dip of the foliations and bedding planes of the Lesser and Higher Himalayan rocks using the Freiberg clinometer compass. At least five measurements are taken at every location and the average of them has been reported in Fig. 4a. Field photos in the supplement (fig. S4-S17) support observed variations in the structural styles.

3.2.2. Rock strength data

Recording rock strength data in the field is important to understand the role of variable rock-type and rock-strength in changes in morphology. It provides us important insights on the genesis of knickpoints whether they are lithologically-controlled or not. It also helps to understand the variations in channel steepness across rocks of similar lithological strength. We systematically measured the rock strength of the main geologic units using a hand-held rebound hammer. Repeated measurements (8-10 measurements at each of the 96 locations throughout the study area) were conducted to measure the variability of rock-strength within the main lithologic units and between them (Fig. 3a). Average rock strength data collected from each of the test locations are plotted against the longitudinal river profile and channel width data in Fig.3b.

4. Results

https://doi.org/10.5194/esurf-2020-37
Preprint. Discussion started: 18 June 2020

Earth Surface Dynamics Discussions

4.1.Field observations and measurements

The Chenab River has deeply incised the KW (*Fig. 2a* and *3c*). The LHS rock units exposed within the KW are mainly composed of Rampur Quartzites and phyllites. with occasional schists in between. (Steck, 2003; Gavillot et al., 2018). The LHD has been suggested to be an asymmetric antiformal stack with a steeper western flank (dip: 70°/west) (*Fig.4a*). The KW is surrounded by rock units related to the Higher Himalayan high-grade metasedimentary sequence, mainly garnet-bearing mica schists and gneisses. Higher Himalayan rocks close to the western edge of the KW form a syncline with a southwest-verging MCT at its' base. The KT, southern structural boundary of the window margin, accommodating the differential exhumation between window internal and surroundings – and it is expressed as highly deformed sub-vertical shear bands.

Along the traverse of the Chenab River through the window and further downstream, two prominent stretches of ~20 and ~25-30 km length have been identified where the channel gradients are high and we observed sequence of rapids (*fig. S5*). These steep segments are also characterized by a very narrow channel width (< 30m) (*fig. S8*). The steepened segments define knickzone rather thana single knickpoint. The knickzones in the trunk stream as well as in the tributaries are hosted over bedrock gorges – and field evidence confirms that none of them (downstream from the eastern edge of the KW) are related to damming by landslides or other mass movements. The eastern margin of the KW is characterized by a wide 'U-shaped' valley filled with thick sand layers and coarser fluvioglacial sediments. The river incises through this Late Pleistocene fill at present (*fig. S4*).

The rock strength data taken along the Chenab trunk stream shows large variations (R-value ranging from 28 to 62) across different morphotectonic segments (*Fig.3a*, *Fig. 3b*). Within

https://doi.org/10.5194/esurf-2020-37
Preprint. Discussion started: 18 June 2020

the KW, Lesser Himalayan phyllites and schists have low R values (30-35); however, the low-strength schists and phyllites are sparsely present. The dominant Rampur quartzites in KW,the , as well as the granitic intrusives in the eastern part of the KW, shows very high R values of 55-62 and 51-56 respectively (*Fig. 3a*). Compared to the high R values in the KW, the Higher Himalayan rocks near the KT (western margin of the KW) show low strength (R: 35-45) till the point L2 (*Fig. 3b*). The rock strength increases (R: 45-50) further downstream until it reaches the MCT shear zone. The R-value in the frontal Lesser Himalaya is moderate (R: 40-45).

The Higher Himalayan sequence dips steeply away from the duplex (~65° towards west) *(fig. S10)*. The frontal horses of the LH duplex expose internally-folded greenschist facies rocks. Although at the western margin of the duplex, the quartzites stand sub-vertically, the general dip amount reduces as we move from west to east for the next ~10-15 km (*Fig. 4a*). Near the core of the KW, we observed deformed quartz veins of at least two generations, as well as macroscopic white mica. Near the core of the window, where the river is also very steep and narrow, the rock units are also steeply-dipping towards the east (~60-65°) and are extremely nearly isoclinal and vigorously deformed at places (*fig. S14, S15*). Towards the eastern edge of the window, however, the quartzites dip much gently towards the east (~25-30°) and much lesser folding and faulting have been recognized in the field.

The E-W traverse of the Chenab river is completely devoid of any sediment storage. However, along the N-S traverse parallel to the western margin of the KW, a sedimentary record for at least one large-scale mass movement have been stored. The debris flow deposits overlie the Higher Himalayan bedrock and another sequence of late Pleistocene fluvioglacial deposits. The town of Kishtwar is situated on this debris flow deposit (*fig. S17*). Along the N-S traverse of the Chenab, we have observed at least two epigenetic gorges lying along the main channel (*fig. S18*). The active channel has incised the Higher Himalayan bedrock and formed strath surfaces.

4.2. Results from morphometric analysis

4.2.1. Steep stream segments and associated knickpoints

The longitudinal stream profile along the Chenab River does not portray a typical adjusted concave-up profile across the Himalaya (*Fig. 2a*). We observe breaks in slope and concavity at least at four occasions within a ~150 km traverse upstream from the MBT. These breaks are defined as knickpoints or knickzones depending on their type characteristics. The slope breaks define the upstream reaches of the steep stream segments. The basinwide steepness indices span from ~30- >750 $m^{0.9}$ across the study area (*Fig. 3a*). We assigned a threshold value of k_{sn}>650 for the steepest watersheds/ stream segments. Along the traverse, the major knickpoints are L1 (~1770m), K1 (~1700m), K2 (~1150m) and L2 (~800m) respectively (*Fig.2a*).

Already Nennewitz et al., (2018) had proposed a high basin-averaged k_{sn} value of > 300 in the KW. Here in this study, we worked with a much-detailed DEM and stream-specific k_{sn} allocation (fig. S3), as well as a basinwide steepness calculation. Our results corroborate with the earlier findings, but, predicts the zone of interest in greater detail. It is important to note that by setting a higher tolerance level in the ‘knickpointfinder’ tool in Topotoolbox, we have managed to remove the DEM artifacts from consideration (Schwanghart and Scherler, 2014).

4.2.2. Channel width and valley morphology

The channel width of the Chenab river is on average low (30-60m) within the core of the KW (*Fig. 3b*), and the low channel width continues till the Chenab River flows N-S along the western margin of the KW. However, there are a few exceptions; upstream from the knickpoint

https://doi.org/10.5194/esurf-2020-37
Preprint. Discussion started: 18 June 2020

L1 in the Padder valley (in which the town of Padder is located), the channel widens (width ~80-100m) and the channel gradient is low (*Fig. 2a*). The second instance of a wider channel is seen upstream from knickpoint K2, where there is a reservoir for the Dul-Hasti dam (*fig. S7*). Downstream from K2 within the Higher Himalaya, the channel width ranges from 50-70 m. However, towards the lower stretches of the N-S traverse, the width is even lower (16-52m). The river width increases to 100-200m as Chenab River takes a westward path thereafter. The river width increases beyond 300m until it leaves the crystalline rocks in the hanging wall of the MCT and enters the Lesser Himalaya in the hanging wall of the MBT across the Baglihar dam. Within the frontal LH, the channel width is again lowered (50-80 m).

We have also drawn topographic swath profiles across the Chenab River, which represents the shape of the valley at four different morphotectonic domains (*Fig.3c*). While section 1 representing the upstream segment of the MCT hanging wall (E-W traverse of the river) shows an 'open' 'V-shaped' profile, the shape of the valley at location 2 across the N-S traverse of the river shows an acute 'V-shaped' channel morphology. The similar strongly-incised channel is seen at the core of the KW (location 3) and location 4 in the Padder valley, where the valley becomes 'U-shaped.'

4.2.3. Changes in specific stream power (SSP)

Discharge-normalized SSP data calculated from the upstream stretches and the knickzones, K1 and K2 show major increase in SSP within the steep knickzones. The increase in SSP from upstream to the knickzones K1 and K2 are 4.44 and 5.02 times, respectively (Table 1). Such high increase in SSP is aided by steepening of channel gradient and narrowing of channel bed.

https://doi.org/10.5194/esurf-2020-37
Preprint. Discussion started: 18 June 2020

5. Discussions

Morphometric parameters are widely used as indicators of active tectonics and transient topography (Hack, 1973; Kirby and Whipple, 2012; Seeber and Gornitz (1983)). Many studies have used morphometry as a proxy for understanding the spatial distribution of active deformation across certain segments of the Himalayan front (Malik and Mohanty, 2007; van der Beek et al., 2016; Nennewitz et al., 2018; Kaushal et al., 2017). More importantly, some studies have integrated morphometric analysis with rigorous chronological constraints to assess the spatial and temporal variability in deformation within the Sub-Himalaya (Lave and Avouac, 2000; Thakur et al., 2014; Vassalo et al., 2015; Dey et al., 2016; Srivastava et al., 2018). All these studies have shown that morphometric indicators can also be used for a qualitative estimate of changes in uplift rate or spatial variations of deformation, even in the Sub-Himalayan domain where the rivers are often alluviated due to high sediment load (Malik and Mohanty, 2007). Therefore, using morphometric indices to examine some prospect areas and using their relative difference as a proxy of relative changes in faulting and differential uplift as well as connecting these regions with nearby regions having chronological constraints on short-intermediate timescale deformation, is a potent option, when applied carefully.

The KW exhibits younger Apatite fission-track cooling ages (~2-3 Ma) as compared to the surrounding Higher Himalaya, which have been interpreted as the result of rapid exhumation of the LH duplex over 10^6-year timescale (Kumar et al., 1995) are higher compared to surrounding Higher Himalaya. However, we lack any measurements of deformation on the 10^3-10^5-year timescale. With the existing AFT data and assuming that no major changes of the deformation regime have taken place since the Quaternary, we may well use it for calibration of

https://doi.org/10.5194/esurf-2020-37
Preprint. Discussion started: 18 June 2020

morphometric proxies and interpolate these estimates to regions, where no thermochronological constraint exists. Thus, we have come up with a morphometric analysis of the terrain and combined those results with existing chronology and structural data as a proxy for the spatial distribution of faulting and fault patterns.

5.1. Knickpoints and their genesis

Already Seeber and Gornitz (1983) showed that the Chenab River is characterized by a zone of steep channel gradient in the vicinity of the KW. Thiede and Ehlers (2013) demonstrated a strong correlation between steeped longitudinal river profiles and young thermochronological cooling ages, suggesting recent focused rock uplift and rapid exhumation along many major rivers draining the southern Himalayan front. Although, it is still an open debate whether uplift and growth of the LHD are triggered solely by slip over the crustal ramp of the MHT or additional out-of-sequence surface-breaking faults are augmenting it (Avouac et al., 2001; Herman et al., 2010; Elliot et al., 2016; Whipple et at., 2016).

The longitudinal profile of the lower Chenab traverse (below ~2000 m above MSL) is punctuated by two prominent stretches of knickpoint zones (Fig.2a). Below we will discuss the potential cause of formation of those major knickpoints in the context of detailed field observation, of existing field-collected structural and lithological data, geomorphic features, rock strength and channel width information (*Fig.3b*).

5.1.1. Lithologically-controlled knickpoints

The Himalayan traverse of the Chenab River is characterized by large variations in substrate lithology and rock strength (*Fig.1*, *Fig.2a*). These variations have inflicted their ‘marks’ on the river profile. An instance of soft-to-hard substrate transition happens across the

https://doi.org/10.5194/esurf-2020-37
Preprint. Discussion started: 18 June 2020

knickpoint L1, lying downstream from the Padder valley, at the eastern edge of the KW (*Fig.2a*). Across L1, the river enters the LH bedrock gorge (R value> 50) after exiting the Padder valley filled with unconsolidated fluvioglacial sediments (*fig. S4*). A similar soft-to-hard substrate transition is observed upstream from the MCT shear zone. The corresponding knickpoint L2 represents a change in lithological formation from the sheared and deformed Higher Himalayan crystalline (R value~35-40) to deep-seated Haimantas (R value~40-50). There is no field evidence, such as fault splays or ramps, in support of L2 to be a structurally-controlled one.

5.1.2. Tectonically-controlled knickpoints

Compiling previously-published data on regional tectonogeomorphic attributes (Gavillot et al., 2018) with detailed field documentation of structural styles and tectonic features, we have deciphered the role of rock-uplift and variable structural styles in the interiors of the NW Himalaya. We have found at least two instances where knickpoints are not related to change in substrate, nor are they artificially altered.

The knickzone K1 (~1700 m above MSL) represents the upstream reach of a steepened stream segment of run-length ~18-20 km. The upstream and downstream side of K1 is characterized by a change in the orientation (dip angle) of the foliation of the LH bedrock (*Fig. 4a*). Across K1, the dips of the foliation planes change from ~30° to ~60-65° towards east. K1 also reflects a change in the channel width (*Fig. 3b*). The steep segment exhibits a narrower channel through the core of the LH duplex. Near the end of the steep segment, we observed intensely-deformed (folded and fractured) LH rocks (*fig. S14*). We explain this as evidence of faulting within the LH duplex and the steep stream segment represents the ramp of the fault or fault zone between two duplex nappes (*Fig.4b*). K1 therefore, reflects the transition from flat to ramp of the existing structure soled to the basal decollement. The steep segment represents a

https://doi.org/10.5194/esurf-2020-37
Preprint. Discussion started: 18 June 2020

Earth Surface Dynamics Discussions Open Access EGU

drop of ~420m of the Chenab river across a run-length of ~20 km (*Fig.2b*). In addition to this, we may comment that the schists and phyllites within the Lesser Himalayan sequence probably act as the basal planes of the thrust nappes.

On the other hand, the other knickpoint K2 nearly coincides with the exposure of the KT (*Fig.2a*). K2 cannot be a lithologically-controlled knickpoint as it reflects a hard-to-soft substrate transition from LH rocks (R value> 50) to HH rocks (R value< 45). However, in the longitudinal profile, K2 does not represent a sharp slope break because the downstream segment runs parallel for ~25-30 km and not perpendicular to the orientation of all major structures of the orogen, including the KT. Therefore, we performed an orthogonal projection of the E-W trending traverses of the Chenab river and tried to estimate an orogen-perpendicular drop of the Chenab across K2 (*Fig. 2c*). The truncated profile across K2 shows a drop of ~230m of the channel across an orogen-perpendicular run-length of ~5 km. The orogen-parallel stretch of the river exhibits narrow channel width (<30-35m) through a moderately hard HH bedrock (R-value: 35-45). The tributaries within this stretch form significant knickpoint at the confluence with the trunk stream (*fig. S6*). These evidences hint towards a rapid uplift of the HH rocks near the western margin of the KT and are possibly related to the presence of another crustal ramp emerging from the MHT (*Fig.4b*).

Both the knickzones, K1 and K2 portray transiently-high specific stream power values (Table 1). This signifies the fact that the knickzones are undergoing much rapid fluvial incision than the rest of the study area. If we consider the fluvial incision as a proxy of relative uplift (assuming a steady-state), we may well say that the knickzones define the spatial extent of the areas undergoing differential uplift caused by movement on the fault ramps.

5.2. Our findings in context with the previously-published data

AFT-cooling ages by Kumar et al., (1995) showcased a rapid exhumation of the KW (AFT ages: ~2-3 Ma) compared to the surroundings (AFT age: 6-12 Ma). Although proper thermal modeling is lacking in this region. Lateral similarities of the regional topography and age patterns along the Sutlej area, Beas and Dhauladhar Range (Thiede et al., 2017; Thiede et al., 2009; Stübner et al., 2018) have yielded 2-3 mm a^{-1} exhumation rates. Long-term exhumation rates from the NW Himalaya agree well with findings of Nennewitz et al. (2018) who correlated the young thermochron ages with high basinwide k_{sn} values suggesting high uplift rates over intermediate to longer timescales. Therefore, the proposed range of long-term exhumation rates of >2 mm a^{-1} determined by Gavillot et al., (2018) agree with the regional data pattern. Although the geomorphic implications on landscape evolution are valid for shorter timescales than the low-T thermochron studies, we must comment that our field observations and analysis support a protracted growth of the LH duplex. Unless there has been a recent growth of the duplex, the geomorphic signatures would have been subdued. Young low-T thermochron ages (Kumar et al., 1995) had been sampled from the steepened stream reaches, where the SSP is high. Interestingly, exhumation rates steepened stretches is ~ten times more than that of the Higher Himalaya in the hanging wall of the duplex. Our estimates of SSP also reflect an increase by ~five times within the steepened stretches.

Deeply-incised channel morphology, steep channel gradients marked by knickpoints at the upstream reaches in and around the KW could be explained by the presence of at least two orogen-parallel mid-crustal ramps on the MHT (*Fig.4b*). Existence of two mid-crustal ramps has already been suggested in the balanced cross-section published by Gavillot et al., (2018). However, the internal structural orientation of the LH duplex published by Gavillot et al., (2018) (*fig. S2*) differ considerably from our field observations (*Supplement 1, part 2*). We observe

https://doi.org/10.5194/esurf-2020-37
Preprint. Discussion started: 18 June 2020

pronounced deformation at the core of the KW suggesting that this is related to active faulting or internal folding at the base of the steepened stretch of K1 (*fig. S16*). The ramp of the fault-zone mentioned above triggers rapid exhumation of the hanging wall. It causes high relief, steep channel gradients and higher basinwide steepness indices over the ramp (*Fig.4a*). Similar ramps have been proposed on the MBT beneath the Dhauladhar Range (Thiede et al., 2017) and in the east of the NW Himalaya (Caldwell et al., 2013; Mahesh et al., 2015; Stübner et al., 2018; Yadav et al., 2019).

Our findings from the Kishtwar region of the NW Himalaya establishes the importance of morphometric parameters in the assessment of intermediate timescales of 10^4-10^6 years. We can resolve variations in the tectonic imprint on landscape evolution by analyzing the topography with high-resolution DEM. Earlier studies used to process larger areas, but the resolution of those data and findings is coarse (Nennewitz et al., 2018).

Models explaining the spatial distribution of the high uplift zone in the interiors of the Himalaya favor the existence of a mid-crustal ramp, which has variable dimension, geometry, and distance from the mountain front along-strike of the Himalayan orogeny (Robert et al., 2009). Our data support the idea of mid-crustal ramps beneath the Higher Himalayan domain (Nennewitz et al., 2018) and we predict that the seismic hypocenters are clustered in the vicinity of the ramp of MHT and within the LHD and are linked to the ongoing growth of the duplex. Our results verify the previously-suggested models that there exist two orogen-parallel small ramps beneath the Kishtwar Window instead of one (Gavillot et al., 2018). However, we must also comment that the previous model as well as the balanced cross-section lack detailing and the thermochron data (Kumar et al., 1995) is sparse. Therefore, field observation and the detailed morphometric analysis using high-resolution DEM help to measure the spatial extent of

https://doi.org/10.5194/esurf-2020-37
Preprint. Discussion started: 18 June 2020

deformation. We are able to resolve the high-relief Kishtwar Window and the surroundings into two major steep orogen-parallel belts/ zones (Fig. 4a). While the larger one is an active high-angle fault-ramp emerging from the MHT and causing sustained uplift in the core of the duplex, the smaller one lies along the western margin of the KW. We suggest that this has two major implications. One, we have evidence for ongoing internal deformation of duplex and that entire window is still growing – and therefor this could be potential source future seismic activity. Two, our finding contradicts with the existence of a single major ramp in the interiors of the Himalaya, as described from other sectors of the Himalaya (Gahalaut and Kalpna, 2001; Elliot et al., 2016; Thiede et al., 2017). This portrays along-strike variations in the geometry of the basal decollement (MHT) in the Himalaya, in agreement with earlier findings.

6. Conclusions

Our field observation and the characteristics of terrain morphology match well with the spatial pattern of previously-published thermochronological data and unanimously indicate that the Kishtwar Window is undergoing active and focused uplift and exhumation at present, during intermediate timescales, and in geological past since at least the late Miocene. By compiling all the results and published records, we favor the following conclusions:

1. The Chenab maintains an over-steepened bedrock and a low channel width irrespective of any lithological variations across the KW and beyond, suggesting ongoing rapid fluvial incision.
2. Our field observations, morphometric analysis, and rock strength measurements document that at least two of these major knickzones on the trunk stream are non-

https://doi.org/10.5194/esurf-2020-37
Preprint. Discussion started: 18 June 2020

lithologic and rather can be related to differential uplift of the rock units. The incision potential in the steepened stretches ~4-5 times higher than the surroundings.

3. The differential uplift is related to variations in the geometry of the basal decollement. Our results show the presence of at least two mid-crustal ramps beneath the Kishtwar Window and the surroundings, as compared to a single crustal ramp proposed from interiors of the nearby sectors of the NW Himalaya.
4. The larger of the proposed crustal ramps emerge as an active high-angle ramp at the core of the Lesser Himalayan Duplex and causes sustained uplift of the hanging wall.

To summarize, our new study reinforces the importance of detailed field observation and morphometric analysis in understanding the neotectonic framework of the interiors of the Himalaya. Our study refutes the long-standing hypothesis of nearly 100% accommodation of late Quaternary crustal shortening within the Sub-Himalayan domain and provides new insights on the structural styles and ongoing deformation in the Himalayan interiors.

Acknowledgments

This study is funded by the DST INSPIRE faculty fellowship program by the Department of Science and Technology, India (grant #DST/INSPIRE/04/2017/003278), and IIT Gandhinagar post-doctoral research fund (IP/IITGN/ES/SD/201718-01). Thiede is supported by German Science Foundation (grant # DFG TH 1317-8 and 9). We thank Shambhu Das, Avi Das, Niklas Schaaf, Akashsingh Rajput and Chamel Singh for their assistance during fieldwork. We also thank Soumyajit Mukherjee, Rahul Kaushal and Shantamoy Guha for scientific inputs and comments on this manuscript.

References

Ahnert, F. (1970). Functional relationships between denudation, relief, and uplift in large, mid-latitude drainage basins. American Journal of Science, 268(3), 243-263.

Bagnold, R. A. (1966). An approach to the sediment transport problem from general physics. US government printing office.

Bhatia, T. R., & Bhatia, S. K. (1973). Sedimentology of the slate belt of Ramban-Banihal area, Kashmir Himalaya. Himalayan Geology, 3, 116-134.

Bollinger, L., Henry, P., & Avouac, J. P. (2006). Mountain building in the Nepal Himalaya: Thermal and kinematic model. *Earth and Planetary Science Letters*, *244*(1-2), 58-71.

Bookhagen, B., Fleitmann, D., Nishiizumi, K., Strecker, M. R., & Thiede, R. C. (2006). Holocene monsoonal dynamics and fluvial terrace formation in the northwest Himalaya, India. *Geology*, *34*(7), 601-604.

Brozovic, N., & Burbank, D. W. (2000). Dynamic fluvial systems and gravel progradation in the Himalayan foreland. GSA Bulletin, 112(3), 394-412.

Burbank, D. W., Leland, J., Fielding, E., Anderson, R. S., Brozovic, N., Reid, M. R., & Duncan, C. (1996). Bedrock incision, rock uplift and threshold hillslopes in the northwestern Himalayas. *Nature*, *379*(6565), 505.

https://doi.org/10.5194/esurf-2020-37
Preprint. Discussion started: 18 June 2020

Burgess, W. P., Yin, A., Dubey, C. S., Shen, Z. K., &Kelty, T. K. (2012). Holocene shortening across the Main Frontal Thrust zone in the eastern Himalaya. Earth and Planetary Science Letters, 357, 152-167.

Caldwell, W. B., Klemperer, S. L., Lawrence, J. F., and Rai, S. S., 2013, Characterizing the Main Himalayan Thrust in the Garhwal Himalaya, India with receiver function CCP stacking: Earth and Planetary Science Letters, v. 367, p. 15-27.

Cortés-Aranda, J., Vassallo, R., Jomard, H., Pousse-Beltrán, L., Astudillo, L., Mugnier, J. L., Jouanne, F., Malik, M., & Carcaillet, J. (2018). Late quaternary out-of-sequence deformation in the innermost Kangra Reentrant, NW Himalaya of India: Seismic potential appraisal from 10Be dated fluvial terraces. Journal of Asian Earth Sciences, 158, 140-152.

DeCelles, P. G., Robinson, D. M., Quade, J., Ojha, T. P., Garzione, C. N., Copeland, P., and Upreti, B. N., 2001, Stratigraphy, structure, and tectonic evolution of the Himalayan fold-thrust belt in western Nepal: Tectonics, v. 20, no. 4, p. 487-509.

Deeken, A., Thiede, R. C., Sobel, E. R., Hourigan, J. K., & Strecker, M. R. (2011). Exhumational variability within the Himalaya of northwest India. Earth Planetry Science Letters, 305(1-2), 103–114. https://doi.org/10.1016/j.epsl.2011.02.045

Dey, S., Thiede, R. C., Schildgen, T. F., Wittmann, H., Bookhagen, B., Scherler, D., & Strecker, M. R. (2016). Holocene internal shortening within the northwest Sub-Himalaya: Out-of-sequence faulting of the Jwalamukhi Thrust, India. Tectonics, 35(11), 2677-2697.

DiPietro, J. A., & Pogue, K. R. (2004). Tectonostratigraphic subdivisions of the Himalaya: A view from the west. Tectonics, 23(5).

https://doi.org/10.5194/esurf-2020-37
Preprint. Discussion started: 18 June 2020

Earth Surface Dynamics
Discussions
Open Access

Duvall, A., Kirby, E., & Burbank, D. (2004). Tectonic and lithologic controls on bedrock channel profiles and processes in coastal California. Journal of Geophysical Research: Earth Surface, 109(F3).

Elliott, J. R., Jolivet, R., González, P. J., Avouac, J. P., Hollingsworth, J., Searle, M. P., & Stevens, V. L. (2016). Himalayan megathrust geometry and relation to topography revealed by the Gorkha earthquake. *Nature Geoscience*, *9*(2), 174.

Eugster, P., Scherler, D., Thiede, R. C., Codilean, A. T., and Strecker, M. R., (2016). Rapid Last Glacial Maximum deglaciation in the Indian Himalaya coeval with midlatitude glaciers: New insights from 10Be-dating of ice-polished bedrock surfaces in the Chandra Valley, NW Himalaya: Geophysical Research Letters, v. 43, no. 4, p. 1589-1597.

Finnegan, N. J., Roe, G., Montgomery, D. R., &Hallet, B. (2005). Controls on the channel width of rivers: Implications for modeling fluvial incision of bedrock. *Geology*, *33*(3), 229-232.

Flint, J. J. (1974). Stream gradient as a function of order, magnitude, and discharge. Water Resources Research, 10(5), 969-973.

Forte, A.M. and Whipple, K.X. (2019). The Topographic Analysis Toolkit (TAK) for Topotoolbox. Earth Surface Dynamics, 7, 87-95.

Gahalaut, V. K., & Kalpna. (2001). Himalayan mid-crustal ramp. *Current Science*, 1641-1646.

Gavillot, Y. G. (2014). Active tectonics of the Kashmir Himalaya (NW India) and earthquake potential on folds, out-of-sequence thrusts, and duplexes.

Gavillot, Y., Meigs, A. J., Sousa, F. J., Stockli, D., Yule, D., & Malik, M. (2018). Late Cenozoic Foreland-to-Hinterland Low-Temperature Exhumation History of the Kashmir Himalaya. Tectonics.

Gavillot, Y., Meigs, A., Yule, Y., Heermance, R., Rittenour, T., Madugo, C., & Malik, M. (2016). Shortening rate and Holocene surface rupture on the Riasi fault system in the Kashmir Himalaya: Active thrusting within the Northwest Himalayan orogenic wedge. Geological Society of America Bulletin, 128(7-8), 1070–1094. https://doi.org/10.1130/B31281.1

Harvey, J. E., Burbank, D. W., & Bookhagen, B. (2015). Along-strike changes in Himalayan thrust geometry: Topographic and tectonic discontinuities in western Nepal. Lithosphere, 7(5), 511-518.

Herman, F., Copeland, P., Avouac, J.P., Bollinger, L., Mahéo, G., Le Fort, P., Rai, S., Foster, D., Pêcher, A., Stüwe, K. and Henry, P., 2010. Exhumation, crustal deformation, and thermal structure of the Nepal Himalaya derived from the inversion of thermochronological and thermobarometric data and modeling of the topography. *Journal of Geophysical Research: Solid Earth*, *115*(B6).

Hirschmiller, J., Grujic, D., Bookhagen, B., Coutand, I., Huyghe, P., Mugnier, J.-L., and Ojha, T., 2014, What controls the growth of the Himalayan foreland fold-and-thrust belt?: Geology, v. 42, no. 3, p. 247-250.

Kaushal, R. K., Singh, V., Mukul, M., & Jain, V. (2017). Identification of deformation variability and active structures using geomorphic markers in the Nahan salient, NW Himalaya, India. *Quaternary International*, *462*, 194-210.

Kumar, A., Lal, N., Jain, A. K., &Sorkhabi, R. B. (1995). Late Cenozoic–Quaternary thermo-tectonic history of Higher Himalayan Crystalline (HHC) in Kishtwar–Padar–Zanskar region, NW Himalaya: Evidence from fission-track ages. Journal of the Geological Society of India, 45(4), 375–391.

Kundu, B., Yadav, R. K., Bali, B. S., Chowdhury, S., &Gahalaut, V. K. (2014). Oblique convergence and slip partitioning in the NW Himalaya: implications from GPS measurements. Tectonics, 33(10), 2013-2024.

Lavé, J., & Avouac, J. P. (2000). Active folding of fluvial terraces across the Siwaliks Hills, Himalayas of central Nepal. Journal of Geophysical Research: Solid Earth, 105(B3), 5735-5770.

Lavé, J., & Avouac, J. P. (2001). Fluvial incision and tectonic uplift across the Himalayas of central Nepal. Journal of Geophysical Research: Solid Earth, 106(B11), 26561-26591.

Mahesh, P., Gupta, S., Saikia, U., and Rai, S. S., 2015, Seismotectonics and crustal stress field in the Kumaon-Garhwal Himalaya: Tectonophysics, v. 655, p. 124-138.

Malik, J. N., & Mohanty, C. (2007). Active tectonic influence on the evolution of drainage and landscape: geomorphic signatures from frontal and hinterland areas along the Northwestern Himalaya, India. *Journal of Asian Earth Sciences*, *29*(5-6), 604-618.

Miller, J. R. (1991). The influence of bedrock geology on knickpoint development and channel-bed degradation along downcutting streams in south-central Indiana. The Journal of Geology, 99(4), 591-605.

https://doi.org/10.5194/esurf-2020-37
Preprint. Discussion started: 18 June 2020

Mitra, G., Bhattacharyya, K., & Mukul, M. (2010). The lesser Himalayan duplex in Sikkim: implications for variations in Himalayan shortening. *Journal of the Geological Society of India*, *75*(1), 289-301.

Montgomery, D. R., & Brandon, M. T. (2002). Topographic controls on erosion rates in tectonically active mountain ranges. Earth and Planetary Science Letters, 201(3-4), 481-489.

Mukherjee S. (2015) A review on out-of-sequence deformation in the Himalaya. In: Mukherjee S, Carosi R, van der Beek P, Mukherjee BK, Robinson D (Eds) Tectonics of the Himalaya. Geological Society, London. Special Publications 412, 67-109.

Mukul, M., Jade, S., Bhattacharyya, A. K., &Bhusan, K. (2010). Crustal shortening in convergent orogens: Insights from global positioning system (GPS) measurements in northeast India. Journal of the Geological Society of India, 75(1), 302-312.

Nábělek, J., Hetényi, G., Vergne, J., Sapkota, S., Kafle, B., Jiang, M., Su, H., Chen, J., & Huang, B. S. (2009). Underplating in the Himalaya-Tibet collision zone revealed by the Hi-CLIMB experiment. Science, 325(5946), 1371-1374.

Nadim, F., Kjekstad, O., Peduzzi, P., Herold, C., &Jaedicke, C. (2006). Global landslide and avalanche hotspots. Landslides, 3(2), 159-173.

Nennewitz, M., Thiede, R. C., & Bookhagen, B. (2018). Fault activity, tectonic segmentation, and deformation pattern of the western Himalaya on Ma timescales inferred from landscape morphology. Lithosphere, 10(5), 632-640.

Ni, J., and M. Barazangi (1984), Seismotectonics of the Himalayan collision zone: Geometry of the underthrusting Indian plate beneath the Himalaya, J. Geophys. Res., 89, 1147 – 1163.

https://doi.org/10.5194/esurf-2020-37
Preprint. Discussion started: 18 June 2020

Paul, H., Priestley, K., Powali, D., Sharma, S., Mitra, S., &Wanchoo, S. (2018). Signatures of the existence of frontal and lateral ramp structures near the Kishtwar Window of the Jammu and Kashmir Himalaya: Evidence from microseismicity and source mechanisms. *Geochemistry, Geophysics, Geosystems*, *19*(9),3097-3114.

Phartiyal, B., Sharma, A., Srivastava, P., & Ray, Y. (2009). Chronology of relict lake deposits in the Spiti River, NW Trans Himalaya: Implications to Late Pleistocene–Holocene climate-tectonic perturbations. *Geomorphology*, *108*(3-4), 264-272.

Powers, P. M., Lillie, R. J., & Yeats, R. S. (1998). Structure and shortening of the Kangra and Dehra Dun reentrants, sub-Himalaya, India. Geological Society of America Bulletin, 110(8), 1010-1027.

Raiverman, V. (1983). Basin geometry, Cenozoic sedimentation and hydrocarbon prospects in north western Himalaya and Indo-Gangetic plains. Petroleum Asia Journal: Petroliferous basins of India, 6(4), 67-92.

Robert, X., Van Der Beek, P., Braun, J., Perry, C., Dubille, M., & Mugnier, J. L. (2009). Assessing Quaternary reactivation of the Main Central thrust zone (central Nepal Himalaya): New thermochronologic data and numerical modeling. *Geology*, *37*(8), 731-734.

Robinson, D. M., & Martin, A. J. (2014). Reconstructing the Greater Indian margin: A balanced cross section in central Nepal focusing on the Lesser Himalayan duplex. *Tectonics*, *33*(11), 2143-2168.

Royden, L., & Taylor Perron, J. (2013). Solutions of the stream power equation and application to the evolution of river longitudinal profiles. *Journal of Geophysical Research: Earth Surface*, *118*(2), 497-518.

https://doi.org/10.5194/esurf-2020-37
Preprint. Discussion started: 18 June 2020

Scherler, D., Bookhagen, B., Wulf, H., Preusser, F., & Strecker, M. R. (2015). Increased late Pleistocene erosion rates during fluvial aggradation in the Garhwal Himalaya, northern India. *Earth and Planetary Science Letters*, *428*, 255-266.

Schwanghart, W., &Scherler, D. (2014). TopoToolbox 2–MATLAB-based software for topographic analysis and modeling in Earth surface sciences. Earth Surface Dynamics, 2(1), 1-7.

Searle, M. P., Noble, S. R., Cottle, J. M., Waters, D. J., Mitchell, A. H. G., Hlaing, T., &Horstwood, M. S. A. (2007). Tectonic evolution of the Mogok metamorphic belt, Burma (Myanmar) constrained by U-Th-Pb dating of metamorphic and magmatic rocks. Tectonics, 26(3).

Seeber, L., &Gornitz, V. (1983). River profiles along the Himalayan arc as indicators of active tectonics. *Tectonophysics*, *92*(4), 335-367.

Snyder, N. P., Whipple, K. X., Tucker, G. E., &Merritts, D. J. (2000). Landscape response to tectonic forcing: Digital elevation model analysis of stream profiles in the Mendocino triple junction region, northern California. Geological Society of America Bulletin, 112(8), 1250-1263.

Steck, A. (2003). Geology of the NW Indian Himalaya. EclogaeGeolHelv, 96, 147-196.

Stevens, V. L., & Avouac, J. P. (2015). Interseismic coupling on the main Himalayan thrust. Geophysical Research Letters, 42(14), 5828-5837.

Strahler, A. N. (1952). Hypsometric (area-altitude) analysis of erosional topography. Geological Society of America Bulletin, 63(11), 1117-1142.

https://doi.org/10.5194/esurf-2020-37
Preprint. Discussion started: 18 June 2020

Stübner, K., Grujic, D., Dunkl, I., Thiede, R., & Eugster, P. (2018). Pliocene episodic exhumation and the significance of the Munsiari thrust in the northwestern Himalaya. *Earth and Planetary Science Letters*, *481*, 273-283.

Thakur, V. C. (Ed.). (1992). Geology of western Himalaya (Vol. 19). Pergamon Press.

Thakur, V. C., Joshi, M., Sahoo, D., Suresh, N., Jayangondapermal, R., & Singh, A. (2014). Partitioning of convergence in Northwest Sub-Himalaya: estimation of late Quaternary uplift and convergence rates across the Kangra reentrant, North India. International Journal of Earth Sciences, 103(4), 1037-1056.

Thiede, R., Robert, X., Stübner, K., Dey, S., &Faruhn, J. (2017). Sustained out-of-sequence shortening along a tectonically active segment of the Main Boundary thrust: The Dhauladhar Range in the northwestern Himalaya. Lithosphere, 9(5), 715-725.

Thiede, R. C., Bookhagen, B., Arrowsmith, J. R., Sobel, E. R., & Strecker, M. R. (2004). Climatic control on rapid exhumation along the southern Himalayan Front. Earth and Planetary Science Letters, 222(3-4), 791–806. https://doi.org/10.1016/j.epsl.2004.03.015

Turowski, J. M., Lague, D., and Hovius, N. (2009). Response of bedrock channel width to tectonic forcing: Insights from a numerical model, theoretical considerations, and comparison with field data. *Journal of Geophysical Research: Earth Surface*, *114*(F3).

Vassallo, R., Mugnier, J. L., Vignon, V., Malik, M. A., Jayangondaperumal, R., Srivastava, P., and Carcaillet, J. (2015). Distribution of the late-Quaternary deformation in northwestern Himalaya. Earth and Planetary Science Letters, 411, 241-252.

https://doi.org/10.5194/esurf-2020-37
Preprint. Discussion started: 18 June 2020

Earth Surface Dynamics Discussions Open Access EGU

Wadia, D. N. (1934). The Cambrian-Trias sequence of north-western Kashmir (parts of Muzaffarabad and Baramula districts). Records of the Geological Survey of India, 68(2), 121-176.

Webb, A. A. G., Yin, A., Harrison, T. M., Célérier, J., Gehrels, G. E., Manning, C. E., & Grove, M. (2011). Cenozoic tectonic history of the Himachal Himalaya (northwestern India) and its constraints on the formation mechanism of the Himalayan orogen. *Geosphere*, *7*(4), 1013-1061.

Wesnousky, S. G., Kumar, S., Mohindra, R., & Thakur, V. C. (1999). Uplift and convergence along the Himalayan Frontal Thrust of India. Tectonics, 18(6), 967-976.

Whipple, K. X., & Tucker, G. E. (1999). Dynamics of the stream-power river incision model: Implications for height limits of mountain ranges, landscape response timescales, and research needs. Journal of Geophysical Research: Solid Earth, 104(B8), 17661-17674.

Whipple, K. X., DiBiase, R. A., & Crosby, B. T. (2013). Bedrock rivers. In Treatise on geomorphology. Elsevier Inc..

Wobus, C. W., Hodges, K. V., & Whipple, K. X. (2003). Has focused denudation sustained active thrusting at the Himalayan topographic front?. *Geology*, *31*(10), 861-864.

Wobus, C., Heimsath, A., Whipple, K., & Hodges, K. (2005). Active out-of-sequence thrust faulting in the central Nepalese Himalaya. Nature, 434(7036), 1008.

Wobus, C., Whipple, K. X., Kirby, E., Snyder, N., Johnson, J., Spyropolou, K., Crosby, B., Sheehan, D & Willett, S. D. (2006). Tectonics from topography: Procedures, promise, and pitfalls. Special papers-geological society of America, 398, 55.

https://doi.org/10.5194/esurf-2020-37
Preprint. Discussion started: 18 June 2020

Yadav, R. K., Gahalaut, V. K., Bansal, A. K., Sati, S., Catherine, J., Gautam, P., Kumar, K., and Rana, N., 2019, Strong seismic coupling underneath Garhwal–Kumaun region, NW Himalaya, India: Earth and Planetary Science Letters, v. 506, p. 8-14.

Yin, A., & Harrison, T. M. (2000). Geologic evolution of the Himalayan-Tibetan orogen. Annual Review of Earth and Planetary Sciences, 28(1), 211-280.

Figure captions

Figure 1: An overview geological map of the western sector of the Indian Himalaya showing major lithology (modified after Steck,2003 and Gavillot et al., 2018) and existing structures (Vassalo et al., 2015; Gavillot et al., 2018). The tectonic Kishtwar Window (KW) is surrounded by exposure of MCT, locally known as the Kishtwar Thrust (KT), and exposes the Lesser Himalayan duplex. The Lesser Himalayan duplex (LH duplex) forms a west-verging asymmetric anticline.

Figure 2: (a) Longitudinal river profile of the Chenab trunk stream showing unadjusted stretches along its traverse through the different morphotectonic sectors of the study region. The profile is color-coded with substrate lithology, and the four knickpoints/zones (K1, K2, L1, L2) observed along profile are color-coded according to their causal factors. (b) and (c) 3-km wide topographic swath profiles drawn across the tectonically-generated knickzones K1 and K2 respectively, show a change in the base level across the steep stream segments. The orthogonal profile projection method has been used in the case of K2 (fig.2c) to identify the width of the steep segment. Importantly, the steep segments portray higher relief and narrow channel width irrespective of lithological variations.

https://doi.org/10.5194/esurf-2020-37
Preprint. Discussion started: 18 June 2020

Figure 3: (a) Basinwide steepness indices map of the study area (plotted using a 1000 km^2 threshold) showing high ksn stretches in and around the KW. Note the high ksn belt at the core of the LH duplex and the western margin of the KW. Rock rebound values (multi-point averaged) collected from the field are plotted alongside. (b) Longitudinal profile of the Chenab trunk stream and associated channel width in and around the KW. Rebound values are extrapolated on the profile. (c) Cross-profile topographic swaths drawn at four locations (shown in fig. 3b) showing variations in channel geometry. Interestingly, the N-S transect of Chenab downstream from the KW shows a narrower channel through a deeply-incised gorge despite weak substrate.

Figure 4: (a) Detailed structural data from the study area showing structural and lithological variations (modified after Steck, 2003; Gavillot et al., 2018). Field evidence for the same are provided in Supplement 1(part 2). (b) A conceptual drawing of the internal deformation of the LH duplex showing the existing structural variations of the MHT and possible locations of mid-crustal ramps. The steep stream segment (~18-20 km long) at the core of the duplex relates to a ramp emerging from the MHT. The folded and fractured LH quartzites at the base of the ramp possibly indicate a surface-breaking fault within the LH duplex. Sustained uplift along the fault cause accentuated uplift of the hanging wall, resulting in higher topographic relief, narrowing of the channel and river steepening indicating a transient topography.

Table caption:

Table 1: Morphometric parameters for calculation of discharge-normalized specific stream power (SSP) in the study area, highlighting the changes in SSP through the steepened stretches. Increase in SSP by 4-5 times through the steepened stretches reflect higher potential for fluvial erosion, balancing the differential uplift of the terrain.

https://doi.org/10.5194/esurf-2020-37
Preprint. Discussion started: 18 June 2020

Earth Surface Dynamics
Discussions
Open Access

Figures

Figure 1

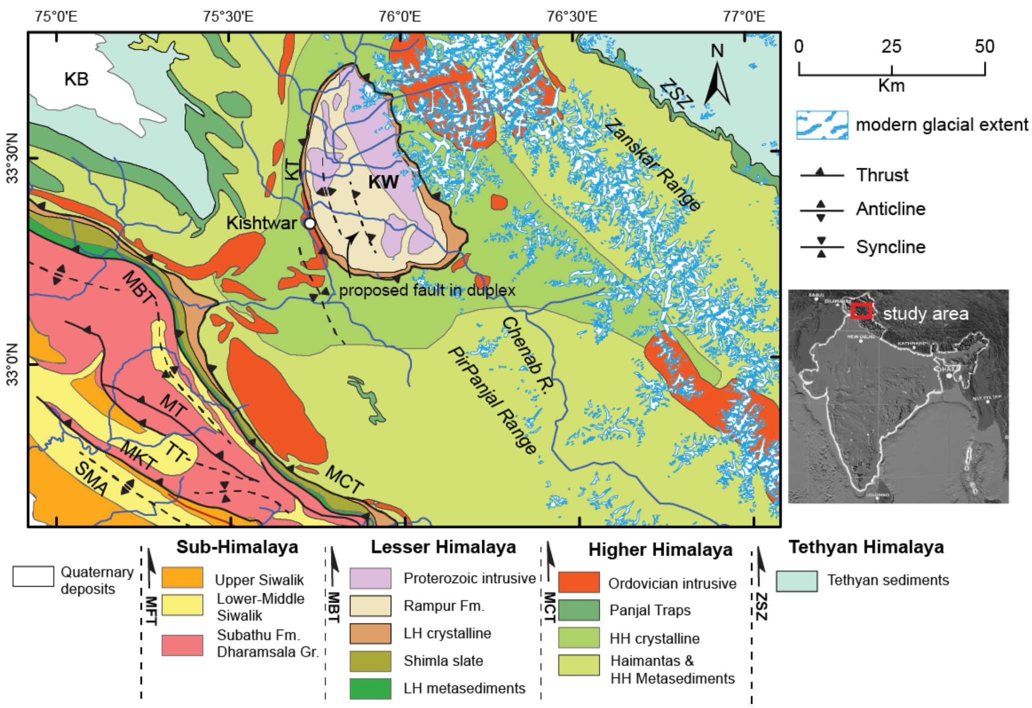

https://doi.org/10.5194/esurf-2020-37
Preprint. Discussion started: 18 June 2020

797 **Figure 2**

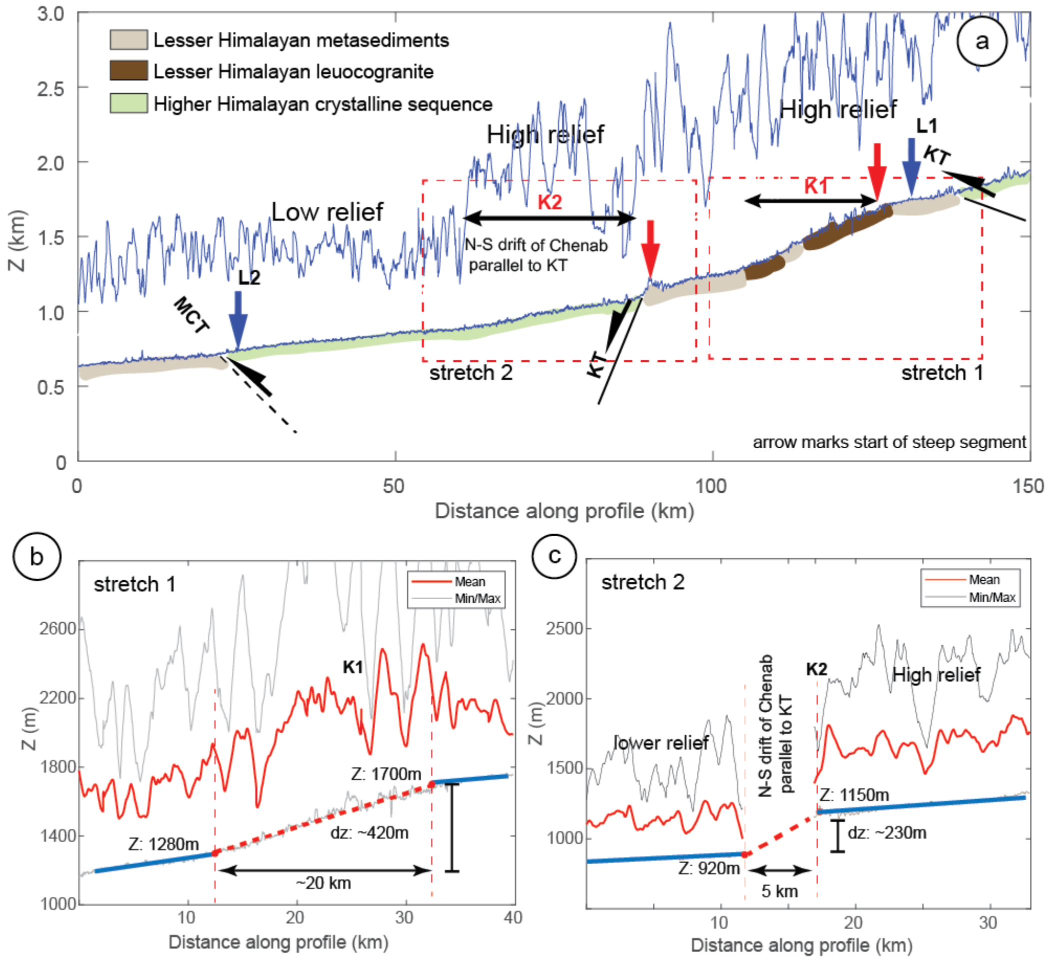

798

799

https://doi.org/10.5194/esurf-2020-37
Preprint. Discussion started: 18 June 2020

Earth Surface Dynamics
Discussions
Open Access
EGU

Figure 3

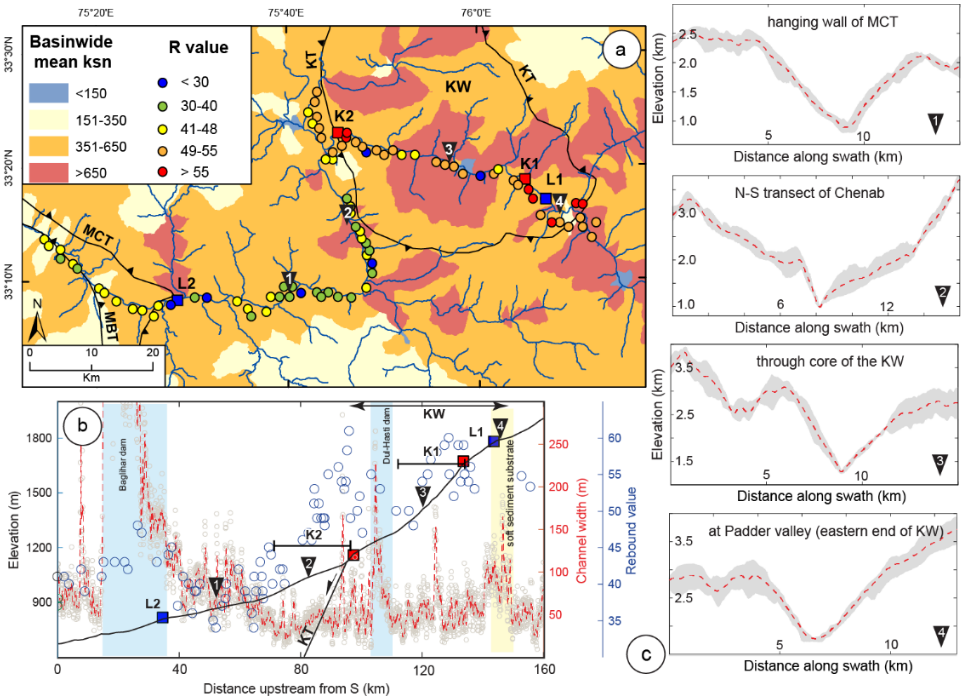

https://doi.org/10.5194/esurf-2020-37
Preprint. Discussion started: 18 June 2020

Earth Surface Dynamics
Discussions
Open Access

Figure 4

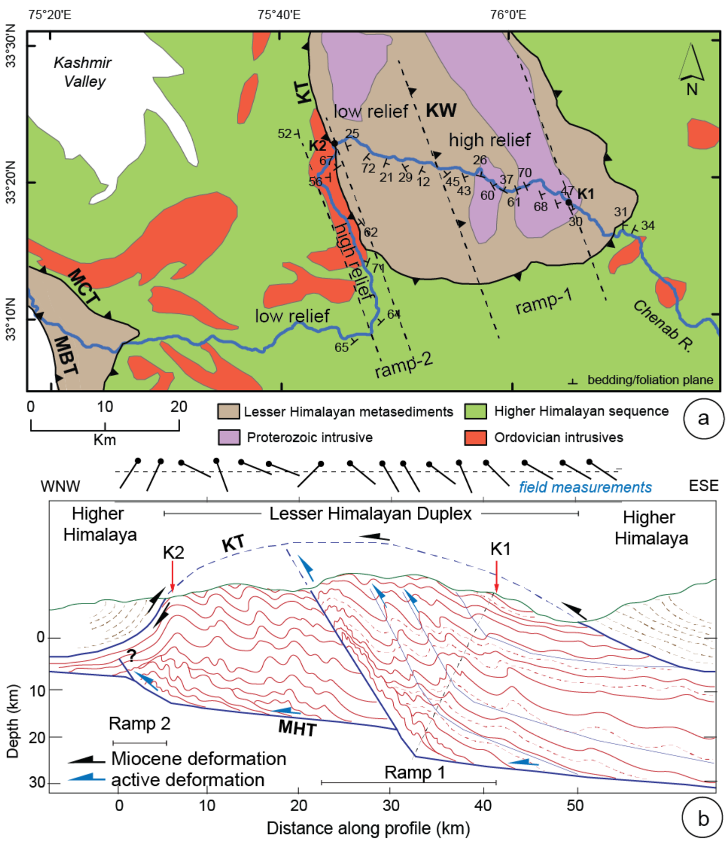

Table 1

Parameter	flat 1	ramp 1	% change	ratio ramp:flat	flat 2	ramp 2	% change	ratio ramp:flat
average channel gradient (m/m)	0.006	0.021	250.00	3.5	0.01	0.046	360	4.60
average channel width (m)	70	45	-35.71	0.6	55	42	-24	0.76
*Specific stream power (SSP)	0.000086	0.000467	444.44	5.4	0.000182	0.001095	502	6.02

* SSP calculated by assuming equal-discharge (Q)